Monthly Notices
of the
ROYAL ASTRONOMICAL SOCIETY

MNRAS **483,** 2185–2196 (2019)
Advance Access publication 2018 November 13

doi:10.1093/mnras/sty3084

The aftermath of the Great Collision between our Galaxy and the Large Magellanic Cloud

Marius Cautun [1]★ Alis J. Deason [1] Carlos S. Frenk[1] and Stuart McAlpine [1,2]

[1]*Department of Physics, Institute of Computational Cosmology, Durham University, South Road, Durham DH1 3LE, UK*
[2]*Department of Physics, University of Helsinki, Gustaf Hällströmin katu 2a, FI-00560 Helsinki, Finland*

Accepted 2018 November 8. Received 2018 October 31; in original form 2018 September 23

ABSTRACT

The Milky Way (MW) offers a uniquely detailed view of galactic structure and is often regarded as a prototypical spiral galaxy. But recent observations indicate that the MW is atypical: it has an undersized supermassive black hole at its centre; it is surrounded by a very low mass, excessively metal-poor stellar halo; and it has an unusually large nearby satellite galaxy, the Large Magellanic Cloud (LMC). Here, we show that the LMC is on a collision course with the MW with which it will merge in $2.4^{+1.2}_{-0.8}$ Gyr (68 per cent confidence level). This catastrophic and long-overdue event will restore the MW to normality. Using the EAGLE galaxy formation simulation, we show that, as a result of the merger, the central supermassive black hole will increase in mass by up to a factor of 8. The Galactic stellar halo will undergo an equally impressive transformation, becoming 5 times more massive. The additional stars will come predominantly from the disrupted LMC, but a sizeable number will be ejected on to the halo from the stellar disc. The post-merger stellar halo will have the median metallicity of the LMC, [Fe/H] $= -0.5$ dex, which is typical of other galaxies of similar mass to the MW. At the end of this exceptional event, the MW will become a true benchmark for spiral galaxies, at least temporarily.

Key words: Galaxy: halo – galaxies: dwarfs – galaxies: haloes – galaxies: kinematics and dynamics – Magellanic Clouds.

1 INTRODUCTION

The Universe is a dynamical system: galaxies are continuously growing and undergoing morphological transformation. For the most part, this is a slow, unremarkable process, but from time to time evolution accelerates through spectacular galaxy mergers. The Milky Way (MW) appears to have been quiescent for many billions of years but its demise has been forecast to occur when, in several billion years time, it collides and fuses with our nearest giant neighbour, the Andromeda galaxy (van der Marel et al. 2012b). This generally accepted picture ignores the enemy within – the Large Magellanic Cloud (LMC).

The LMC is an unusually bright satellite for a MW-mass galaxy: observations indicate that only 10 per cent of galaxies of similar mass have such bright satellites (e.g. Guo et al. 2011; Liu et al. 2011; Robotham et al. 2012; Wang & White 2012). While the LMC has a stellar mass roughly 20 times smaller than our galaxy (van der Marel et al. 2002), it is thought to possess its own massive dark halo. Local Group dynamics as well as abundance matching based on hydrodynamic simulations suggest that the LMC halo mass is around a quarter of the Galactic halo mass (Peñarrubia et al. 2016; Shao et al. 2018). A large total mass is supported indirectly by the complement of satellite galaxies that the LMC is thought to have brought with it into the Galaxy. These satellites-of-satellites include the Small Magellanic Cloud (SMC, the second brightest Galactic dwarf), and a large fraction of the recently discovered satellites in the Dark Energy Survey (e.g. Kallivayalil et al. 2013; Deason et al. 2015; Jethwa, Erkal & Belokurov 2016; Sales et al. 2017; Kallivayalil et al. 2018).

The atypical brightness of the LMC is just one of the several features that make our galaxy stand out. For its bulge mass, the MW has a supermassive black hole whose mass is nearly an order of magnitude too small (Savorgnan et al. 2016). The growth of supermassive black holes results from a complex interplay between host halo mass, gas supply, and stellar and AGN feedback: in low mass haloes, $\lesssim 10^{12}\,\mathrm{M}_{\odot}$, stellar feedback is efficient at regulating the central gas content and black holes hardly grow; in more massive haloes, the stellar feedback-driven outflow loses its buoyancy, and stalls, triggering the rapid growth phase of the central black hole (e.g. Booth & Schaye 2010, 2011; Dubois et al. 2015; McAlpine et al. 2016; Anglés-Alcázar et al. 2017; Bower et al. 2017). Furthermore, mergers also play a crucial role by enhancing black hole growth (e.g. Volonteri, Haardt & Madau 2003; Hopkins et al. 2005;

★ E-mail: m.c.cautun@durham.ac.uk

Di Matteo et al. 2008; Goulding et al. 2018; McAlpine et al. 2018). Thus, the low mass of the MW black hole could be a consequence of a low halo mass and the scarcity of mergers experienced by our galaxy.

The stellar halo of the MW is also atypical, being very metal poor and of rather low mass (e.g. Merritt et al. 2016; Monachesi et al. 2016a; Bell et al. 2017; Harmsen et al. 2017). Stellar haloes typically grow through mergers and the tidal disruption of satellites, and thus provide a unique insight into a galaxy's assembly history (e.g. Bullock & Johnston 2005; Cooper et al. 2010, 2015; Rodriguez-Gomez et al. 2016). Dwarf galaxies exhibit a strong correlation between stellar mass and metallicity (e.g. Kirby et al. 2013), a relation that is reflected in the stellar haloes of larger galaxies, with higher mass objects being more metal rich (e.g. Monachesi et al. 2016b, 2018; D'Souza & Bell 2018b). Besides the accreted component, stellar haloes are also predicted to have an *in situ* component that formed in the main galaxy rather than in a satellite and was ejected into the halo (e.g. Brook et al. 2004; Zolotov et al. 2009; Font et al. 2011; Tissera et al. 2013; Cooper et al. 2015; Pillepich, Madau & Mayer 2015). However, the significance of this component in the MW is still under debate (e.g. Helmi et al. 2011; Bonaca et al. 2017; Deason et al. 2017; Haywood et al. 2018).

The low mass and high radial concentration of the Galactic stellar halo could indicate that the MW has grown slowly through minor mergers since redshift, $z \sim 2$, and that its dark matter halo formed early (e.g. Deason et al. 2013; Deason, Mao & Wechsler 2016; Amorisco 2017a,b). Indeed, recent studies using *Gaia* astrometric data have shown that the last major accretion event likely occurred between 8 and 11 Gyr ago, around the time when the Galactic disc was beginning to form (Belokurov et al. 2018; Helmi et al. 2018).

In this paper we investigate the probable orbital evolution of the LMC and find that it is on a collision course with the MW. We then use the state-of-the-art EAGLE galaxy formation simulation (Schaye et al. 2015) to predict how the outcome of the LMC merger will change the MW. In particular, we focus on the evolution of the stellar halo and the central supermassive black hole of our galaxy, the two components that make the MW so atypical when compared to other spiral galaxies of similar stellar mass. Both of these components are known to be affected by mergers, raising an intriguing question: After the merger with the LMC, will the MW remain an outlier in so far as its black hole and stellar halo are concerned?

Coincidently, our neighbour, Andromeda, presents a very informative picture of the merger process between a massive dwarf and a MW-sized galaxy. Andromeda is thought to be in the late stages of such a merger, in which the Giant Southern Stream and M32 are a tidal stream and the core of a merging dwarf at least as massive as the LMC (e.g. Fardal et al. 2006, 2013; D'Souza & Bell 2018a).

This paper is organized as follows: Section 2 presents an orbital evolution model for the Local Group and its application to the future evolution of the MW–LMC–Andromeda system; Section 3 introduces a sample of MW–LMC analogue systems identified in the EAGLE simulation and an analysis of their evolution; Section 4 offers a prediction for the post-LMC merger properties of the MW central supermassive black hole and stellar halo; and finally, Section 5 presents the conclusions of our study.

2 THE FUTURE OF THE MW–LMC SYSTEM

We use a semi-analytic model of the orbital dynamics of the Local Group to study the future evolution of the MW–LMC system. We start by presenting a detailed description of the orbital model, followed by the most likely predictions for the evolution of the Local Group.

Table 1. The masses of the dark matter halo ($M_{200}^{\rm DM}$), bulge ($M_{\rm bulge}$), and disc ($M_{\rm disc}$) of the MW, LMC, and Andromeda (M31) used in our orbital model. We use two dynamical models that differ only by the mass, $M_{200}^{\rm DM}$, assigned to the LMC halo. The *fiducial LMC model*, which corresponds to the Peñarrubia et al. (2016) mass determination, is the more realistic one and is the one used for our predictions. The *light LMC model* corresponds to the minimum halo mass given the LMC rotation curve (Gómez et al. 2015) and is used to illustrate the effect of a low LMC halo mass. The future evolution of the MW–LMC–Andromeda system for the two models is shown in Fig. 1. The errors are 1σ uncertainties and are used for calculating the uncertainties in the future evolution of the MW–LMC system. The halo masses are masses contained within the region whose mean density is 200 times the critical density.

Galaxy	$M_{200}^{\rm DM}$ $[\times 10^{12}\,{\rm M}_\odot]$	$M_{\rm bulge}$ $[\times 10^{10}\,{\rm M}_\odot]$	$M_{\rm disc}$ $[\times 10^{10}\,{\rm M}_\odot]$
MW	$1.00^{+0.25}_{-0.25}$	1.0	4.5
M31	$1.30^{+0.35}_{-0.35}$	1.5	10.3
Fiducial LMC model			
LMC	$0.25^{+0.09}_{-0.08}$	0.27	–
Light LMC model			
LMC	0.05	0.27	–

2.1 Dynamical model

We predict the future orbital evolution of the LMC using a semi-analytic model for the Local Group orbital dynamics, which we take to be composed of the MW, LMC, and Andromeda. The MW and Andromeda are modelled as having three components: a dark matter halo, a bulge, and a disc, while the LMC is modelled as having only a dark matter halo and a bulge. The masses of the various components of the three galaxies are listed in Table 1 and correspond to: MW, LMC, and Andromeda halo masses from Peñarrubia et al. (2016); MW bulge and disc masses from McMillan (2017); Andromeda bulge and disc masses from Savorgnan et al. (2016); and LMC stellar mass from van der Marel et al. (2002). In particular, our assumed MW halo mass is in very good agreement with the recent determination using *Gaia* data by Callingham et al. (2018), as well as with other measurements (see e.g. fig. 7 of Callingham et al.). Furthermore, the assumed LMC halo mass is in good agreement with the estimate by Shao et al. (2018), as well as with our own determination based on the EAGLE simulation (see Section 3.1).

We model the dark matter halo as a sphere with the Navarro, Frenk, and White density profile (Navarro, Frenk & White 1996, 1997, hereafter, NFW), whose potential is given by

$$\Phi_{\rm halo} = -\frac{G M_{200}^{\rm DM}}{r} \frac{\log\left(1 + c\, r/R_{200}\right)}{\log(1+c) - c/(1+c)}\,, \tag{1}$$

where c is the concentration parameter, $M_{200}^{\rm DM}$ is the dark matter halo mass, and R_{200} is the halo radius. The concentrations of the NFW haloes are taken as the median concentrations for their mass, which are $c = 7$ for the MW and Andromeda, and $c = 8$ for the LMC (Hellwing et al. 2016); the assumed concentration makes little difference to the model outcome since the uncertainties are dominated by the halo mass and LMC proper motion errors. The potentials of the two baryonic components are modelled as a Hernquist bulge

(Hernquist 1990),

$$\Phi_{\rm bulge} = -\frac{G M_{\rm bulge}}{r + r_{\rm c}}\,, \tag{2}$$

where $M_{\rm bulge}$ and $r_{\rm c}$ are the bulge mass and scale radius, respectively, and a Miyamoto–Nagai disc (Miyamoto & Nagai 1975)

$$\Phi_{\rm disc} = -\frac{G M_{\rm disc}}{\sqrt{R^2 + \left(r_{\rm a} + \sqrt{Z^2 + r_{\rm b}^2}\right)^2}}\,, \tag{3}$$

where $M_{\rm disc}$ is the disc mass and $r_{\rm a}$ and $r_{\rm b}$ are the scale lengths. The symbols R and Z denote the radial and vertical cylindrical coordinates, respectively, while r denotes the distance. For the MW, we take the following constant values of the bulge and disc scale lengths: $r_{\rm c} = 0.7$ kpc, $r_{\rm a} = 3.5$ kpc, and $r_{\rm b} = 0.53$ kpc (Gómez et al. 2015). For simplicity, we adopt the same bulge and disc scale lengths for Andromeda; however, these values do not affect the outcome of the MW–LMC merger.

We implement dynamical friction as a deceleration experienced by the lower mass galaxy when orbiting within the virial radius of the more massive companion. We assume that the deceleration is given by Chandrasekhar's formula (Binney & Tremaine 2008),

$$\frac{{\rm d}\mathbf{v}}{{\rm d}t} = -\frac{4\pi G^2 M \rho \ln\Lambda}{v^2}\left[{\rm erf}(X) - \frac{2X}{\sqrt{\pi}} e^{-X^2}\right]\frac{\mathbf{v}}{v}\,, \tag{4}$$

where M is the satellite mass, $\mathbf{v}$ is the relative velocity of the satellite and the host halo, ρ denotes the density of the host at the satellite's position, and $X = v/(\sqrt{2}\sigma)$, with σ the local 1D velocity dispersion of the host halo. We take the Coulomb factor as $\Lambda = r/\varepsilon$, where r is the instantaneous separation between satellite and host, and ε is a scale length that depends on the density profile of the satellite. We take the value of ε from Jethwa et al. (2016), who performed N-body simulations of the MW–LMC systems for a set of MW and LMC halo mass values. The value of ε that best reproduces the LMC orbit in the Jethwa et al. N-body simulations is

$$\epsilon = \begin{cases} 2.2 r_{\rm s} - 14\,{\rm kpc} & \text{if } r_{\rm s} \geq 8\,{\rm kpc} \\ 0.45 r_{\rm s} & \text{if } r_{\rm s} < 8\,{\rm kpc} \end{cases}\,. \tag{5}$$

We position the three galaxies (MW, Andromeda, and LMC) at the centre of their haloes and start the orbit integration using the present-day position and velocities, which we take from the McConnachie (2012) compilation. When calculating velocities, we adopt the Kallivayalil et al. (2013) proper motion for the LMC and the van der Marel et al. (2012a) value for Andromeda (note that these proper motions are consistent with the recent *Gaia* DR2 estimates; Gaia Collaboration 2018; van der Marel et al. 2018). For each galaxy, we calculate the gravitational pull exerted by the other two companions and, for the LMC, we include the additional deceleration due to dynamical friction (equation 4). We then integrate the equations of motion using a symplectic leapfrog scheme. We define the MW–LMC merger as the moment when the LMC comes within 10 kpc of the MW and, once this has happened, the orbital evolution model treats the MW–LMC system as a single object. This merger threshold is based on EAGLE analogues of the MW–LMC system (see Section 3.2): once the LMC-mass satellite comes within 10 kpc of the central galaxy, it is rapidly tidally stripped and merges with its central galaxy.

To estimate the uncertainties in the orbit of the MW–LMC system, we Monte Carlo sample the estimates of the LMC proper motions and distance from the MW, as well as the dark matter halo masses of the LMC, MW, and Andromeda. (See Table 1 for the halo masses and associated 1σ uncertainties.) We obtain 1000 Monte Carlo realizations of the MW–LMC–Andromeda system and we calculate the evolution of each realization using the semi-analytic orbital evolution model.

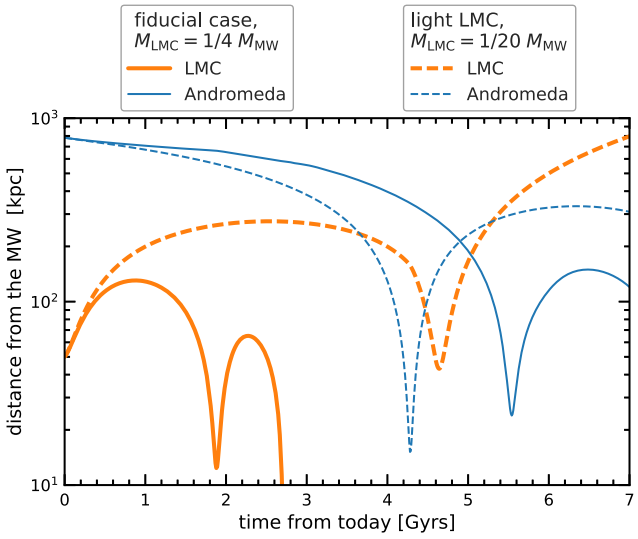

Figure 1. The predicted future evolution of the distance between the LMC and the centre of our Galaxy (orange lines), and between Andromeda and our Galaxy (blue lines). The solid lines correspond to the orbit of our fiducial model in which the LMC's total mass is given by the Peñarrubia et al. (2016) measurement and corresponds to roughly one quarter of the MW's mass; the dashed lines correspond to the orbit for a light LMC halo. The predictions are based on a dynamical model that includes the MW, Andromeda, and the LMC, whose masses are given in Table 1.

2.2 The future evolution of the MW–LMC system

Fig. 1 shows the future time evolution of the distance from the MW of the LMC and Andromeda. For our fiducial model (see Table 1), we find that the LMC is on a radially elongated orbit and will sink towards the Galactic Centre and merge with the MW in 2.7 Gyr. When accounting for observational uncertainties using the Monte Carlos samples described in Section 2.1, we find a most likely merger time of $2.4^{+1.2}_{-0.8}$ Gyr (68 per cent confidence level). Furthermore, this merger will take place many billions of years before the first close encounter between the MW and Andromeda. Unlike the forthcoming merger with Andromeda, the collision with the LMC will not destroy the Galactic disc (see e.g. the case of the Andromeda–M32 merger discussed by D'Souza & Bell 2018a) but could still have immense repercussions for the stellar halo and central supermassive black of our galaxy (see Section 4).

Interestingly, if the LMC were much lighter, it would have been on a very different orbit. To illustrate this, Fig. 1 also shows the orbit corresponding to an LMC halo mass of $5 \times 10^{10}\,{\rm M}_\odot$, which corresponds to the minimum allowed halo mass taking into account the rotation curve of the LMC and the fact that the LMC extends to at least 15 kpc (see e.g. Gómez et al. 2015). A 'light' LMC would have been on a harmless, long period orbit and, possibly, could have been kicked out of the Local Group by the MW–Andromeda merger. However, with a mass as large as indicated by the recent estimates, dynamical friction due to the MW mass distribution will cause the LMC to lose energy leading to a rapid decay of its orbit.

A massive LMC also alters the position and velocity of the barycentre of the MW–LMC system. The change in barycentre affects the orbits of the other satellites (e.g. Gómez et al. 2015; Sohn et al. 2017) as well as the future evolution of the Local Group (Peñarrubia et al. 2016). The change in velocity of the MW–LMC barycentre leads to Andromeda having a larger relative tangential velocity, so that the MW–Andromeda crash will be less head-on than previously predicted. This will also affect the time of the first close encounter between the MW and Andromeda and, for example, for our fiducial model shown in Fig. 1, the first encounter will happen in 5.6 Gyr, which is 1.3 Gyr later than predicted for the low LMC halo mass model. The same result holds true even when accounting for observational uncertainties, for which we predict that the first MW–Andromeda encounter will happen in $5.3^{+0.5}_{-0.8}$ Gyr (68 per cent confidence level), nearly ∼1.5 Gyr later than the $3.9^{+0.4}_{-0.3}$ Gyr value of previous estimates (van der Marel et al. 2012b). Thus, a massive LMC explains away another puzzle: the apparently anomalously low transverse velocity of Andromeda, which is very rare in cosmological simulations (Fattahi et al. 2016). In fact, this is purely a fortuitous occurrence; the transverse velocity will increase as the LMC moves along its orbit.

Fig. 2 illustrates the effect on the inferred LMC and Andromeda orbits of uncertainties in the halo masses of the LMC and the MW. A larger LMC or MW halo mass results in greater dynamical friction and thus a faster merger time-scale for the MW–LMC system. Varying the LMC mass within the 1σ measurement confidence interval adds an uncertainty of ± 0.5 Gyr to the merger time. Varying the MW mass within its 1σ range adds a similar level of uncertainty, ± 0.4 Gyr. Although the LMC and MW halo masses are uncertain at the ∼30 per cent level, we find that the uncertainty in the merger time is dominated by measurement errors in the LMC velocity with respect to the Galactic Centre, which are at the 6 per cent level. When taking into account all these sources of uncertainty, we predict that the MW–LMC merger will take place in $2.4^{+1.2}_{-0.8}$ Gyr (68 per cent confidence level).

To sample the measurement uncertainties, we have obtained 1000 Monte Carlo realizations of the MW–LMC–Andromeda system (see Section 2.1). These show that the MW–LMC merger is a very likely outcome, with the merger taking place in 93 per cent of cases. Of the Monte Carlo realizations that have a MW–LMC merger, 90 per cent have a merger time less than 4 Gyr. Furthermore, in the vast majority of cases (90 per cent), the LMC merges with the MW on its second pericentre passage from today, which corresponds to its third overall pericentre passage as observations suggest that the LMC is currently just past its first pericentre (Kallivayalil et al. 2013).

In 92 per cent of Monte Carlo realizations, the LMC merger takes place before Andromeda has come within 300 kpc of the MW; the presence of Andromeda at such large distances does not affect the LMC–MW merger. This suggests that our omission of M33, which is about twice the mass of the LMC (McConnachie 2012), from the dynamical modelling of the Local Group does not affect our conclusions regarding the MW–LMC merger. However, the M33 galaxy does affect the predictions for the MW–Andromeda collision (for more details, see e.g. van der Marel et al. 2012b; Patel, Besla & Sohn 2017). Furthermore, there are additional sources of uncertainty regarding the MW–Andromeda collision that are not included in our model, such as the uncertainty in the Andromeda proper motion (van der Marel et al. 2012b), which is poorly determined, and the large-scale tidal field in which the Local Group is embedded (Sawala et al, in preparation).

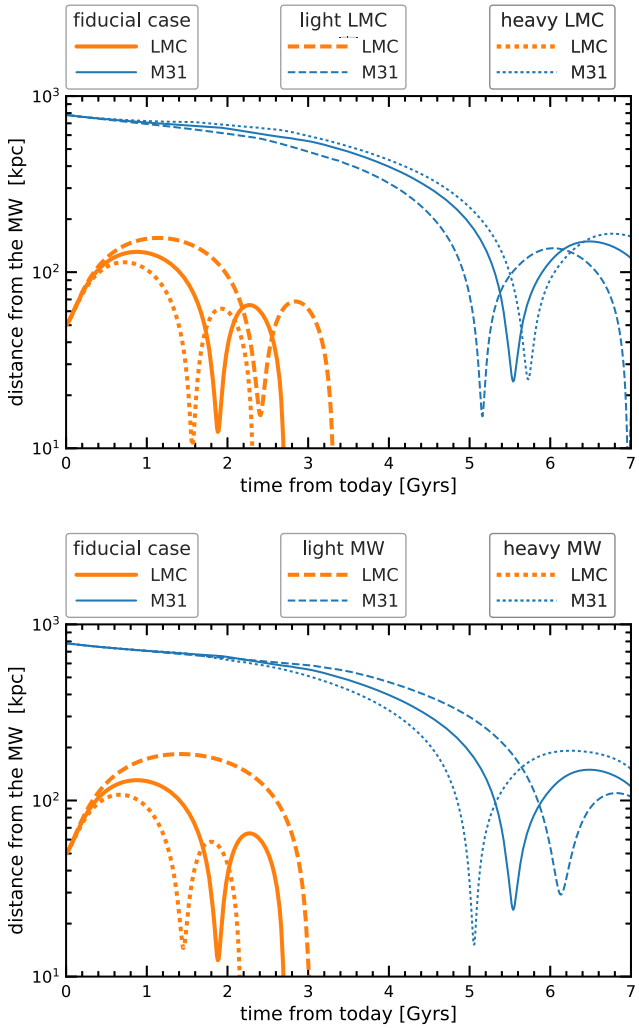

Figure 2. The effect of uncertainties in the total halo masses of the LMC (top panel) and the MW (bottom panel) on the orbits of the LMC and the Andromeda (M31) galaxies. All model parameters are kept to their fiducial values (see Table 1) with the exception of the LMC (top panel) and MW (bottom panel) halo masses. We show the fiducial case as well as results for halo mass values 1σ above and below the most likely estimate. For the LMC, the halo masses are: 2.5 (fiducial), 1.7 (light), and 3.4 (heavy) $\times 10^{11}\,\mathrm{M}_\odot$. For the MW, the halo masses are: 1.0 (fiducial), 0.7 (light), and 1.3 (heavy) $\times 10^{12}\,\mathrm{M}_\odot$.

3 MW–LMC ANALOGUES IN THE EAGLE SIMULATION

To investigate the outcome of the predicted MW–LMC merger, we use the EAGLE suite of cosmological hydrodynamic simulations (Crain et al. 2015; Schaye et al. 2015). EAGLE incorporates the best current understanding of the physics of galaxy formation, and produces a realistic population of galaxies with properties that match a plethora of observations: sizes, star formation rates, gas content, and black hole masses (e.g. Furlong et al. 2015; Schaye et al. 2015; Trayford et al. 2015; Rosas-Guevara et al. 2016; Bower et al. 2017; McAlpine et al. 2017).

The main EAGLE simulation follows the formation and evolution of galaxies in a periodic cubic volume of 100 Mpc on a side assuming the Planck cosmological parameters (Planck Collaboration I 2014). It employs 1504^3 dark matter particles of mass of $9.7 \times 10^6\ \mathrm{M}_\odot$ and 1504^3 gas particles of initial mass

of 1.81×10^6 M$_\odot$. To study analogues of the MW–LMC merger, we make use of the EAGLE galaxy merger trees built from ∼200 outputs, which roughly corresponds to one snapshot every 70 Myr (McAlpine et al. 2016; Qu et al. 2017).

3.1 LMC total mass estimates from EAGLE

According to recent estimates, the dark matter halo of the LMC is very massive, with a total mass at infall on to the MW of $\sim 2.5 \times 10^{11}$ M$_\odot$ (e.g. Peñarrubia et al. 2016). Here, we check if this mass measurement is consistent with the EAGLE simulation. The EAGLE galaxy mass function at stellar masses of 10^9–10^{10} M$_\odot$ matches observations very well (see fig. 4 in Schaye et al. 2015) and thus EAGLE is suitable for inferring the typical halo mass of LMC-mass galaxies.

To estimate the LMC halo mass at infall, we need to determine the time when it first crossed the virial radius of the MW and its stellar mass at that time. We ran the semi-analytic orbit evolution model backwards to trace the infall orbit of the LMC. Our fiducial model predicts that the LMC is on first infall (in agreement with, e.g. Besla et al. 2007; Kallivayalil et al. 2013), just past its first pericentre, and that it recently entered the MW halo, having arrived within 300 kpc comoving distance of our Galaxy for the first time only 1.6 Gyr ago. Within the last 2 Gyr, the LMC had an average star formation rate of 0.2 M$_\odot$ yr^{-1} (Harris & Zaritsky 2009), and thus, at infall 1.6 Gyr ago, the LMC had a stellar mass of 2.4×10^9 M$_\odot$, which is 10 per cent lower than its current value.

Under the assumption that, at infall, the LMC was typical of central galaxies of that stellar mass, we use the redshift, $z = 0.13$, snapshot of the EAGLE reference simulation to identify LMC analogue central galaxies, which we define as having a stellar mass in the range (2–4) $\times 10^9$ M$_\odot$. Our selection criterion returned 1714 LMC-mass central galaxies that have a stellar-to-total mass ratio of $1.23^{+0.53}_{-0.29} \times 10^{-2}$ (68 per cent confidence level). This corresponds to an LMC halo mass at infall, $M_{200} = 1.9^{+0.7}_{-0.7} \times 10^{11}$ M$_\odot$ (68 per cent confidence level), about 30 per cent lower, but still consistent to within 1σ, with the Peñarrubia et al. (2016) measurement.

However, the LMC is not a typical dwarf galaxy. It has a very massive satellite, the SMC, which is the second largest satellite of the MW, with a stellar mass of about a third of the LMC's (McConnachie 2012). This motivated us to identify in EAGLE LMC-mass central galaxies that have an SMC-mass satellite. We define SMC analogues as satellite galaxies with a stellar mass between 0.25 and 0.5 times that of their LMC-mass central galaxy. LMC-mass central galaxies that contain an SMC-mass satellite are rare; we found only 26 examples in EAGLE. However, these binary systems are 1.55 times more massive than the typical LMC-mass central galaxy and have a stellar-to-total mass ratio of $0.79^{+0.28}_{-0.15} \times 10^{-2}$ (68 per cent confidence level). This suggests that the LMC is very massive, with a total halo mass of $M_{200} = 3.0^{+0.7}_{-0.8} \times 10^{11}$ M$_\odot$ (68 per cent confidence level), in good agreement with the Peñarrubia et al. (2016) result, but now roughly 20 per cent higher.

3.2 Selection of MW–LMC analogues

To identify MW–LMC analogues in EAGLE, we started by selecting all the dark matter haloes with a present-day mass in the range (0.5–3.0) $\times 10^{12}$ M$_\odot$, and followed their merger trees to identify satellite galaxy mergers. We restricted attention to mergers that took place between 1 and 8 Gyr ago; the lower bound is needed to be able to estimate the properties of the system some time after the merger, while the upper bound corresponds to redshift, $z = 1$. We found that the resulting central black hole mass after the merger was correlated with several central and satellite galaxy properties. The black hole grew more when: (1) the merging satellite was more massive; (2) the central galaxy had more cold gas; (3) the initial black hole mass was lower; and (4) the merger was not preceded by another LMC-sized merger within a few gigayears. This and other considerations motivated us to adopt the following criteria for identifying analogues that best match the MW–LMC system:

(i) The merging satellite should have a stellar mass in the range (2–4) $\times 10^9$ M$_\odot$, which corresponds to a small interval around the LMC estimated stellar mass of 2.7×10^9 M$_\odot$.

(ii) The central galaxy one dynamical time before the merger should have a cold gas mass of at least 6×10^9 M$_\odot$, which is motivated by H I and molecular gas observations of the MW (Heyer & Dame 2015).

(iii) The central galaxy black hole mass one dynamical time before the merger should be in the range (2–8) $\times 10^6$ M$_\odot$, which is a factor of 2 either side of the value measured for the MW (Boehle et al. 2016).

(iv) The merger with the LMC analogue must not have been preceded by another merger within the last 5 Gyr with a satellite of stellar mass 1×10^9 M$_\odot$ or higher. This is motivated by the absence of such recent mergers in the MW.

The dynamical time provides a characteristic time-scale for the merger, which increases as the Universe ages and which we take to be the gravitational free-fall time, $t_{\rm dyn} = \frac{3\pi}{32 G \overline{\rho}}$, where G is the gravitational constant and $\overline{\rho}$ is the mean density of the system. These selection criteria resulted in eight MW–LMC analogues whose properties are detailed in Table 2. Most analogues correspond to mergers that took place ∼7 Gyr ago, with only one system experiencing a more recent merger at 5 Gyr ago. The early merger time is mainly driven by requiring a close match to the mass of the MW black hole, which is very low when compared to present-day galaxies in both observations and the EAGLE simulation (see Figs 5 and 8). The MW analogues have a stellar mass a factor of a few lower than our Galaxy; this is because we are studying the progenitors of present-day MW-mass galaxies, and, in addition, EAGLE underpredicts the central stellar mass of galactic mass haloes by a factor of 2 (see e.g. Schaye et al. 2015).

To disentangle the effects of the merger with an LMC-sized satellite from those due to passive evolution, we selected a control sample of matched merger-free galaxies. For each MW–LMC analogue, we identified all the galaxies that, in the time interval $[-2t_{\rm dyn}, +2t_{\rm dyn}]$ around the time of the merger, have not themselves undergone a merger with a satellite of stellar mass larger than 1×10^8 M$_\odot$. We further selected only the top merger-free galaxies that have the closest values of dark matter halo, stellar, black hole, and gas masses to the corresponding MW analogues. In total, the control sample contains 40 galaxies, 5 for each MW–LMC analogue system.

3.3 The merger of MW–LMC analogues

Fig. 3 illustrates the evolution of the eight MW–LMC analogues we found in EAGLE. Each analogue has a label, from 1 to 8, with 1 corresponding to the system in which the merger triggered the largest increase in the mass of the central black hole, and 8 to the system that experienced the smallest increase in black hole mass. The top-left panel in Fig. 3 shows the evolution of the central black hole mass from one dynamical time before the merger to one dy-

Table 2. Select properties of the eight MW–LMC analogue systems identified in the EAGLE simulation. The analogues have the same label as in Figs 3 and 4. The columns give: the lookback time, $t_{\rm merger}$, when the merger took place; the stellar, black hole, and cold gas mass, and the bulge-to-total, B/T, ratio of the central galaxy at one dynamical time before the merger; and the maximum stellar mass of the LMC analogue.

		MW analogue				LMC analogue
Analogue ID	$t_{\rm merger}$ [Gyr]	$M_\star$ [$\times 10^{10}\,{\rm M}_\odot$]	$M_{\rm BH}$ [$\times 10^{6}\,{\rm M}_\odot$]	$M_{\rm gas}$ [$\times 10^{10}\,{\rm M}_\odot$]	B/T	$M_\star$ [$\times 10^{9}\,{\rm M}_\odot$]
1	7.8	1.5	4.4	1.1	0.34	3.9
2	6.1	2.0	4.2	1.0	0.29	2.8
3	7.1	0.9	3.0	0.7	0.88	2.6
4	7.6	1.1	5.5	0.8	0.74	4.0
5	4.8	2.6	4.3	0.9	0.36	2.5
6	7.7	1.5	6.8	0.8	0.43	2.2
7	7.7	1.9	4.9	1.0	0.24	3.3
8	6.1	3.3	7.4	1.0	0.13	3.8

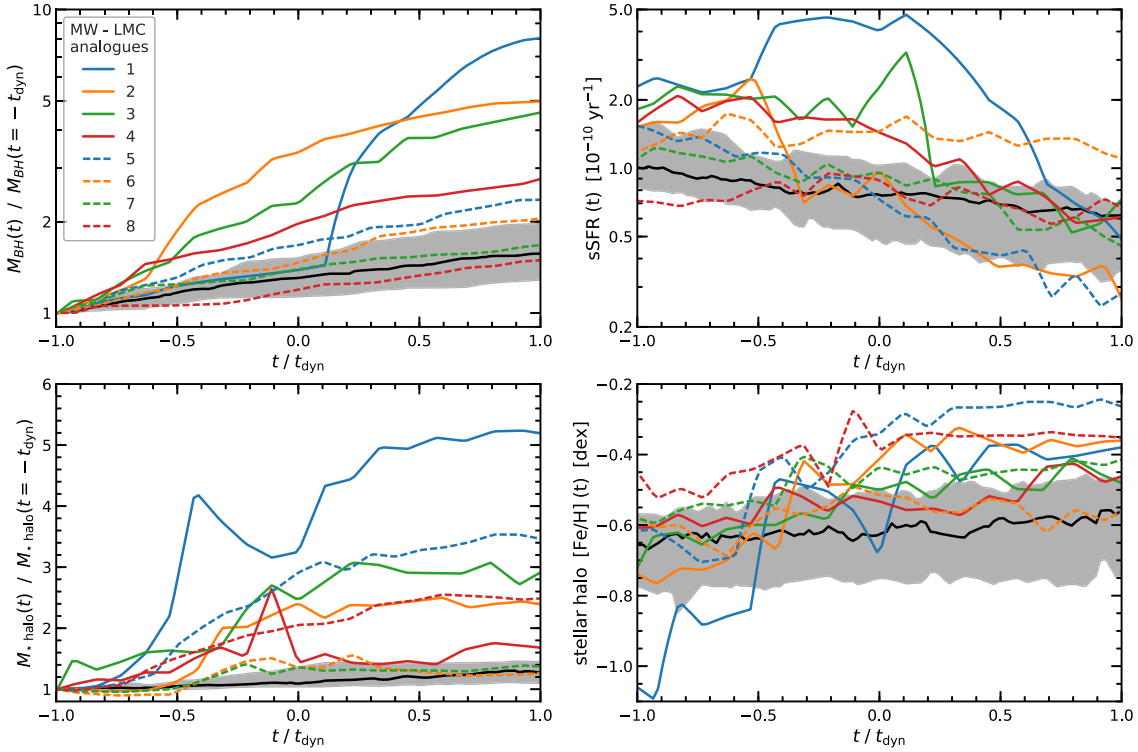

Figure 3. Time evolution around the merger time of the eight MW–LMC analogues found in the EAGLE simulation. The horizontal axis shows time in units of the dynamical time, $t_{\rm dyn}$, when the merger took place, with zero corresponding to the time of the merger. The panels show: the relative increase in central black hole mass (top-left); the specific star formation rate of the central galaxy (top-right); the relative increase in stellar halo mass (bottom-left); and the metallicity of the stellar halo (bottom-right). The colour curves show the evolution of the eight MW–LMC analogues. The black curve and the grey shaded region show the median and the 1σ scatter for the merger-free control sample.

namical time after the merger. The final black holes ended up having masses between 1.5 and 8 times (median value 2.6) the initial values. To put this into perspective, we can compare with the evolution of a control sample of similarly selected MW-mass galaxies that did not experience any massive satellite mergers (Section 3.2). Within the same time frame, the black hole mass of the control sample increased on average by just a factor of 1.5. This underlines the critical role of mergers as triggers of black hole growth (e.g. McAlpine et al. 2018). In particular, this shows that even minor mergers, in this case with mass ratios around 1 : 20, can trigger significant black hole growth. The enhanced black hole growth is due to the merger giving rise to asymmetric disturbances in the central galaxy, which drain angular momentum from the gas of the central galaxy, and drive it into the centre where the black hole resides (Mihos & Hernquist 1996). The gas brought in by the merging satellite represents only a small fraction of the cold gas already present in the central galaxy and is not the primary driver of the black hole growth.

The large increase in the central black hole mass of the MW analogues raises an important question: Would this trigger powerful AGN activity? In EAGLE, the growth of black holes is accompanied by AGN activity, with the injected feedback energy being directly proportional to the recent black hole mass accretion rate (Schaye et al. 2015). To investigate to what extent AGN activity is

enhanced during the MW–LMC merger, we calculate the black hole luminosity for both the MW–LMC analogues and the control sample following equation (1) from McAlpine et al. (2017), whereby we assume a radiative efficiency of 10 per cent (Shakura & Sunyaev 1973). We find that all eight analogues show vigorous AGN activity between one dynamical time before and after the merger. AGNs brighter than 10^{43} erg s^{-1} are active for a fraction of 0.15–0.40 of the time, with the highest fraction corresponding to systems with the largest black hole mass growth. For example, the top four MW–LMC analogues in terms of black hole mass growth (their black hole masses increased during the merger by more than a factor of 2.5) have a 10^{43} erg s^{-1} or brighter AGN for a fraction of 0.3–0.4 of the time around the merger. This represents a factor of a few times enhancement in AGN activity compared to the control sample, which have similarly bright AGN luminosities for a fraction of only 0.05–0.2 of the time (see McAlpine et al. 2018, for a more detailed analysis of merger-induced AGN activity in EAGLE).

The top-right panel in Fig. 3 shows that, except for one case, the specific star formation rate (sSFR) of the central galaxy remains roughly flat during the merger. The sSFR, averaged over the interval of one dynamical time before and after the merger, takes values from 0.5 to 1.2 (median value 0.75) times the sSFR at one dynamical time before the merger. This is in contrast to the MW–Andromeda collision, where previous studies predicted that the star formation rate would roughly double during the merger (Cox & Loeb 2008). Compared to the control sample, which was selected to have the same amount of cold gas, the MW–LMC analogues have slightly higher star formation rates; this enhancement is seen long before the actual merger with the LMC analogue. Thus, the present-day MW could also have a higher sSFR than typical spiral galaxies, which do not have an LMC-sized satellite. However, we note that the potential enhancement of the sSFR is relatively weak.

The bottom row in Fig. 3 shows the evolution of the mass and metallicity of the stellar halo during the merger. To calculate the stellar halo mass, we counted all the star particles located between 10 and 100 kpc from the central galaxy (Bell et al. 2017) and excluded any stars that were part of bound substructures. The calculation excludes disc stars that are found beyond 10 kpc by removing any star that orbits within 30° of the central disc plane, and then correcting the resulting mass estimate for the missing angular region by assuming isotropy. The merger of the LMC satellite analogue can result in a large increase in stellar halo mass.[1] The variation in fractional mass increase is mainly driven by the variation in the initial mass of the stellar halo, with low-mass systems having the largest fractional mass increase. For example, the MW–LMC analogue labelled number 1 has an initial stellar halo mass of 5×10^8 M$_\odot$, approximately equal to the present-day Galactic stellar halo mass, and its mass is 5 times larger after the merger.

We also followed the evolution of the stellar halo metallicity at 30 kpc from the central galaxy, which corresponds to the typical distance at which the metallicity is measured from observations (see e.g. Monachesi et al. 2016a; Bell et al. 2017). To calculate this quantity, we selected halo stars using the same procedure as for the stellar halo mass calculation, but now applied to the radial range 20–40 kpc. The bottom-right panel in Fig. 3 shows that an LMC-mass merger leads to an increase in the stellar halo metallicity, with the largest increase occurring in the systems with the largest stellar halo mass growth. The metallicities of dwarf galaxies in EAGLE are too high (Schaye et al. 2015) which, in turn, leads to more metal-rich stellar haloes than found in observations (see Fig. 6). This is not a problem here since in Fig. 3 we are only concerned with relative changes. Furthermore, when extrapolating the MW–LMC analogue results to the real MW, we use the observed metallicities of the MW and LMC, not the EAGLE ones.

To make predictions relevant to the actual MW–LMC merger, we tracked the stars belonging to the satellite and central galaxy analogues (within 10 kpc in the latter case), and identified the stars that one dynamical time after the merger had ended up as part of the stellar halo. As in the bottom row of Fig. 3, we excluded stars that orbit within 30° of the plane of the central disc, correcting the resulting mass estimate by assuming that the halo is isotropic. The results are shown in the top panel of Fig. 4, where we express the increase in the stellar halo mass as a fraction of the LMC analogue stellar mass. On average, the stellar halo grows by a factor of 0.8 of the LMC mass, but the exact values can vary from 0.35 to 1.0. Most of the growth results from tidal stripping of the merging satellite, but there are also central disc stars that are gravitationally ejected into the halo. In the case of analogue number 3, the mass growth

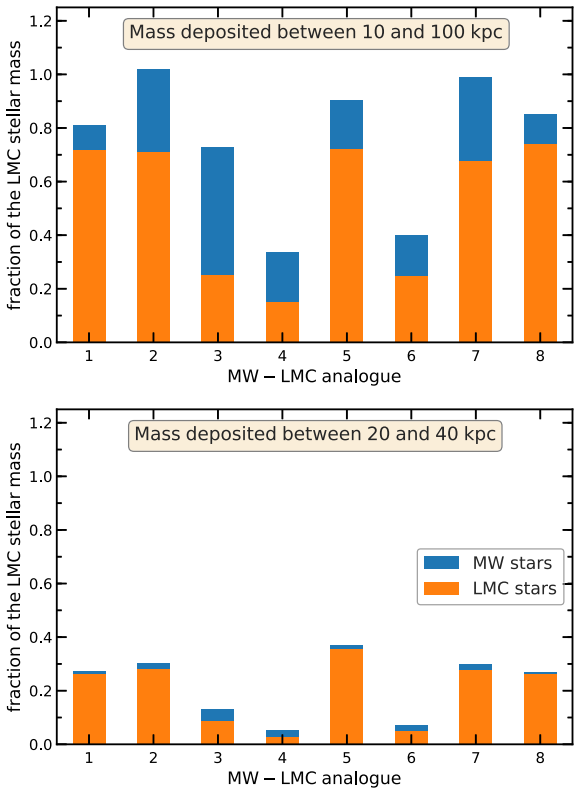

Figure 4. The increase in the stellar halo mass expressed as a fraction of the stellar mass of the LMC analogue. Plotted is the mass deposited in the stellar halo between 10 and 100 kpc (top panel) and between 20 and 40 kpc (bottom panel). The increase due both to stars that were initially part of the LMC analogue (orange) and to stars that were initially part of MW analogue (blue) is shown. Each column corresponds to a MW–LMC analogue, in the same order as in Fig. 3.

[1]The large transient peaks seen in the evolution of the stellar halo mass of systems 1 and 4 correspond to simulation outputs where the structure-finding algorithm wrongly assigns most of the satellite mass to the central galaxy, which can happen when the satellite is very close to the central galaxy (see Qu et al. 2017, for more details).

is dominated by central galaxy stars, but this is more the exception than the rule.

In the top panel of Fig. 4 three MW–LMC analogue mergers stand out: systems 4 and 6, whose stellar halo grows only by 0.4 times the mass of the merging satellite, and system 3, in which most of the stellar halo mass growth is due to stars kicked out from the central galaxy. Systems 4 and 6 correspond to mergers in the plane of the disc and thus, by excluding stars with orbits in the plane of the disc, we do not take into account the mass deposited within this region. System 3 corresponds to a bulge-dominated central galaxy (bulge-to-total ratio of 0.88) and the plane in which the merger takes place becomes the new plane of the post-merger low-mass disc. None of these three systems resembles the MW in terms of bulge-to-disc ratio (∼0.2 for our Galaxy), or in terms of the merging satellite orbit (the LMC orbit is nearly perpendicular to the MW disc). In contrast, the other five EAGLE systems are closer MW–LMC analogues: all five central galaxies are disc dominated (bulge-to-total ratios less than 0.36) and the growth of the stellar halo mass in all five is similar to that of EAGLE systems 5 and 8, which have merging satellite orbits nearly perpendicular to the central disc.

We also calculated the increase in stellar halo mass between 20 and 40 kpc, which is the radial range we used to estimate the increase in stellar halo metallicity (at 30 kpc from the central galaxy). This is shown in the bottom panel of Fig. 4. In contrast to the top panel, the growth of the stellar halo in this region is much less than in the inner region, with only 20 per cent of the stellar mass of the LMC analogue being deposited in the 20–40 kpc shell. Thus, most of the increase in stellar halo mass takes place in the inner regions (Cooper et al. 2010, 2015; Amorisco 2017a) and central disc stars are mainly ejected just outside the 10 kpc radius, with very few reaching a distance of 20 kpc or more (Cooper et al. 2015).

4 THE MW BEFORE AND AFTER THE LMC MERGER

We now investigate the impact of the LMC merger on the mass of the central black hole and the properties of the stellar halo of our galaxy. For this, we consider the eight MW–LMC analogues identified in the EAGLE simulation that we described in Section 3.

4.1 The evolution of the central black hole

Fig. 5 shows the well-known relationship between the mass of the central supermassive black hole and the stellar mass of the spheroid for a large sample of nearby galaxies (e.g. Kormendy & Richstone 1995; Magorrian et al. 1998). The large scatter around the mean trend results from a combination of measurement errors and a 0.5 dex intrinsic scatter (Savorgnan et al. 2016). The black hole of the MW is plotted as a star. Its mass, $(4.0 \pm 0.2) \times 10^6\,\mathrm{M}_\odot$ (Boehle et al. 2016), is 8 times smaller than expected from the mean central black hole–spheroid mass relation. This anomaly is very unlikely to be due to measurement errors alone: the MW is a 2σ outlier in the relation. The lightness of the MW black hole is even more striking when compared to Andromeda which, for a spheroid that is 1.5 times more massive, has a black hole that is 35 times more massive.

To estimate the MW black hole mass after the LMC merger, we used the eight MW–LMC analogues in the EAGLE simulation. In all these systems, the merger caused a large increase in the mass

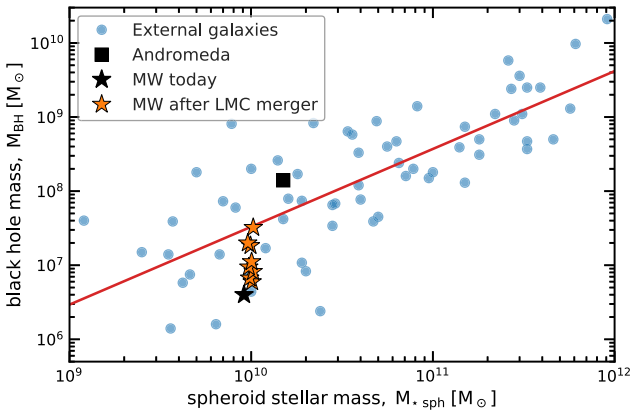

Figure 5. The relation between the mass of the central supermassive black hole and the stellar mass of the spheroid. The relation for a sample of external galaxies (Savorgnan et al. 2016) is shown by filled circles; the current values for the MW and Andromeda are shown by the black star and the black square, respectively. The solid line is the best-fitting power law to the mean relation. Measurement errors vary in size from galaxy to galaxy and, for clarity, are not shown, but they were used in the determination of the mean relation. The orange stars show the evolution of the MW–LMC analogues identified in the EAGLE simulation and represent the likely distribution of values for the MW after the merger with the LMC.

of the central black hole, with the post-merger black holes having masses between 1.5 and 8 times the initial values. We assume that these mass growth rates are typical of MW–LMC mergers, and thus we expect that the mass of our Galaxy's black hole will increase by a similar factor.

To predict how the Galactic black hole will evolve in Fig. 5, we also estimated the MW spheroid mass post-LMC merger in the EAGLE analogues. In the period between one dynamical time before and after the merger, the average sSFR of the eight MW analogues was 0.5–1.2 times the sSFR at one dynamical time before the merger. We use these values, together with the present-day sSFR of the MW (Bland-Hawthorn & Gerhard 2016), 0.03 Gyr^{-1}, to estimate the likely MW stellar mass growth from the present day until the LMC merger occurs. On average, in the next 3 Gyr, the MW stellar mass will grow by 7 per cent. We also find that the bulge-to-disc ratio for the eight MW analogues identified in EAGLE remains constant during the LMC merger. Thus, the LMC merger will preserve the MW disc and will not lead to a considerable growth of the MW bulge (D'Souza & Bell 2018a have found a similar result for the Andromeda merger with M32). A constant bulge-to-disc ratio means that the stellar mass growth during the merger is proportionally split between the two components, and thus the mass of the bulge and the disc grows by the same factor.

The predicted position in the black hole–spheroid mass diagram of the post-merger MW is shown in Fig. 5 with orange star symbols, where each point has been scaled according to the growth seen in each of the eight MW–LMC analogues identified in EAGLE. We find that mergers give rise to significant black hole growth without a corresponding increase in spheroid mass. This is exactly the trend needed to bring the MW black hole into closer agreement with the average black hole–spheroid mass relation. Curiously, Andromeda appears to have had a recent, possibly still ongoing, merger with the massive satellite, M32 (Fardal et al. 2013; D'Souza & Bell 2018a), that may explain why its black hole is so much more massive than the MW's. In particular, the satellite merger in Andromeda seems to have left the stellar disc mostly unharmed, although slightly

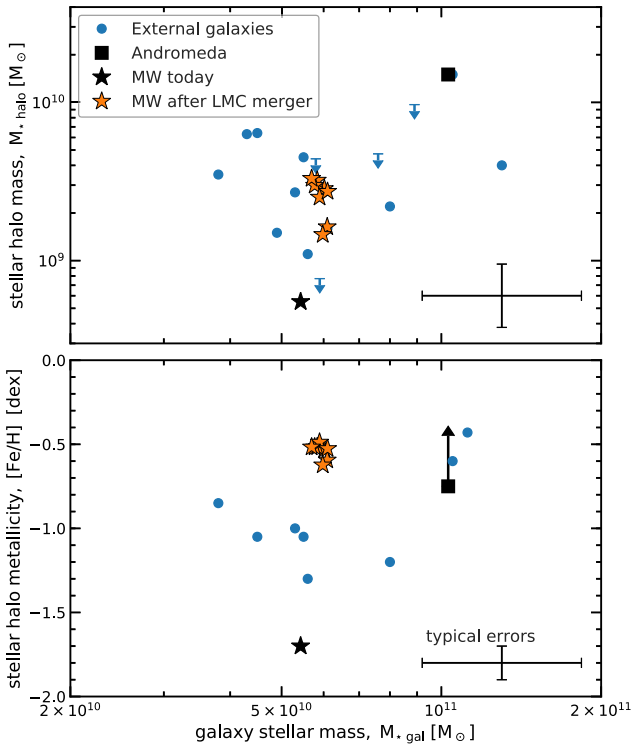

Figure 6. The relation between the galaxy stellar mass and the mass (top panel) and metallicity (bottom panel) of the stellar halo for a sample of nearby galaxies (filled circles) (Bell et al. 2017). The measured values for the MW and Andromeda are shown by a black star and black square, respectively. Upper limits on stellar halo mass are shown by a downward-pointing arrow. The square in the right-hand panel shows the metallicity of Andromeda's smooth stellar halo; when accounting for substructures the median [Fe/H] value (Gilbert et al. 2014) is possibly as high as −0.4 dex, as indicated by an upward-pointing arrow. The orange stars show the likely distribution of final locations for the MW after the merger with the LMC and are derived from the outcome of similar mergers in the EAGLE simulation.

puffed-up, in good agreement with our finding that the MW–LMC merger will not destroy our galactic disc (e.g. see also Gómez et al. 2016, 2017).

4.2 The evolution of the stellar halo

The anomalously low mass and iron abundance of the stellar halo of the MW are clearly apparent in Fig. 6 where the properties of the MW are compared with those of a sample of nearby galaxies (Bell et al. 2017). There is considerable system-to-system variation but, most strikingly, the MW is an extreme outlier, with a very low mass and very metal-poor stellar halo. This is in stark contrast with Andromeda, which has a particularly massive and metal-rich stellar halo.

We use the evolution of the stellar haloes of the MW–LMC analogues to predict the expected mass and metallicity of the Galactic halo after the LMC merger. According to the top panel of Fig. 4 the merger caused an increase in the mass of the stellar halo by a factor between 0.35 and 1.0 of the stellar mass of the merging satellite. The mass of the MW's stellar halo, 0.55×10^9 M$_\odot$ (Bell et al. 2017), is much smaller than the stellar mass of the LMC, 2.7×10^9 M$_\odot$, so the LMC merger will result in the Galactic stellar halo becoming 3–6 times (median value 5) more massive than before the merger.

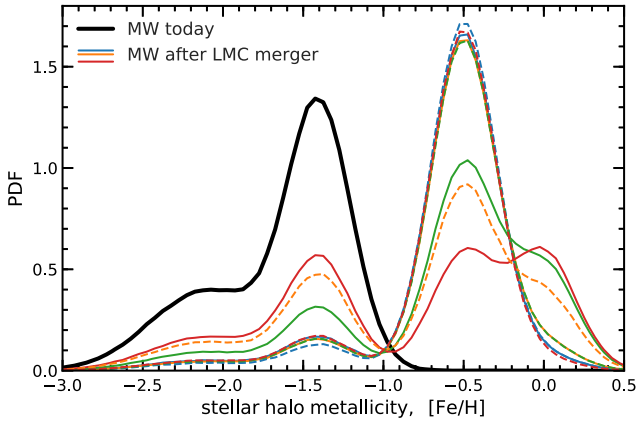

Figure 7. The probability distribution function of the metallicity of the Galactic stellar halo following the merger with the LMC. The present-day metallicity distribution (Xue et al. 2015) is shown as a thick black line and the possible outcomes after the LMC merger as colour lines corresponding to each of the eight MW–LMC analogues; the colour scheme is as in Fig. 3.

This increase would place the MW right in the middle of the stellar halo mass distribution (see the top panel of Fig. 6), turning our galaxy into a 'typical' object.

To predict the metal abundance, [Fe/H], of the post-merger Galactic stellar halo, we use the stellar halo mass growth rates of the MW–LMC analogues at 30 kpc. We model the post-merger stellar halo as having three distinct stellar populations: the present-day population of halo stars, stars stripped from the LMC, and stars ejected from the MW disc. These are mixed according to the mass contributed by each of the three components. The iron abundance of the present-day halo stars is well described by two Gaussians with peaks at −1.4 and −2.1 and widths of 0.2 and 0.35, respectively (Xue et al. 2015). This is shown as the thick solid line in Fig. 7. The LMC and MW iron abundances were modelled as Gaussians with 0.2 dispersion and mean values of −0.5 and 0.0, respectively (McConnachie 2012; Hayden et al. 2015).

The possible [Fe/H] distributions of the MW stellar halo after the LMC merger are shown in Fig. 7, where each curve corresponds to the weighted sum of the metallicities of LMC and MW stars at 30 kpc inferred from the eight EAGLE MW–LMC analogues (see the bottom panel of Fig. 4). Following the merger, the LMC stars will dominate the halo and thus the median [Fe/H] value will be close to that of the present-day LMC. However, the distributions vary somewhat amongst the analogues, with three cases showing a bump at [Fe/H] = 0.0 dex corresponding to MW disc stars and also a sizeable fraction of present-day halo stars. These three cases are the ones in the bottom panel of Fig. 4, which have the smallest increase in stellar halo mass.

The predicted median metallicity of the post-merger Galactic halo is shown as the set of orange star symbols in the bottom panel of Fig. 6, each corresponding to one of the eight MW–LMC EAGLE analogues. Since most of the stellar halo mass growth is due to stripped LMC stars, the median stellar halo iron abundance is similar to that of the LMC, [Fe/H] = −0.5 dex, but the exact value varies somewhat from one MW–LMC analogue to another. The predicted post-merger MW stellar halo is somewhat more metal rich than the comparison sample of local galaxies. The stellar halo reflects the metallicity of its most massive progenitor; the LMC has had longer to evolve and thus to increase its metallicity than the most massive stellar halo progenitors of other nearby galaxies.

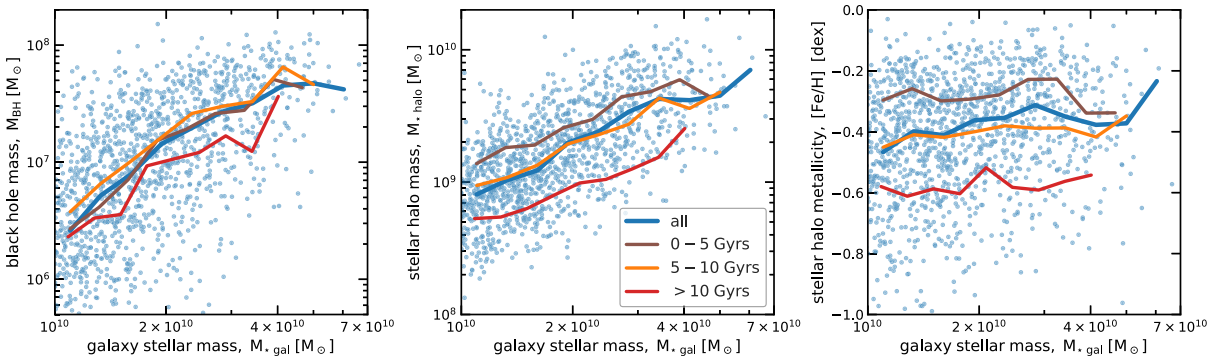

Figure 8. The correlation between present-day central galaxy properties and the lookback time to the last significant merger in the EAGLE simulation. The three panels show, respectively, the black hole mass, the stellar halo mass, and the halo metallicity, as a function of the galaxy stellar mass. The points show individual EAGLE galaxies residing in MW-sized dark matter haloes. The lines show the median trend for all galaxies (blue) and for subsamples split according to the lookback time to the last merger with a satellite more massive than the SMC: 0–5 Gyr (brown), 5–10 Gyr (orange), and >10 Gyr (red).

Comparing to Andromeda, which experienced a very recent merger, we find that when stellar substructures are included the median metallicity of the Andromeda stellar halo at 30 kpc could be as high as −0.4 dex (Gilbert et al. 2014), very similar to our prediction for the post-merger MW.

4.3 The effect of mergers on EAGLE galaxies

We have shown that even 'minor' mergers with LMC-sized satellites can have a large impact on the growth of the central black hole and the stellar halo of MW-sized galaxies. In this paper we have argued that the reason why the MW is an extreme outlier in the properties of these components is a lack of such satellite mergers in the past. The growth of a disc as massive as the MW's, which contains more than 80 per cent of the total galactic stellar mass (McMillan 2017), requires a quiet evolutionary history for the last ∼10 Gyr, with no major mergers and, at most, a few minor ones (Brooks & Christensen 2016). We can resort to the EAGLE simulation to search for correlations between satellite mergers and the final properties of the central galaxy.

Fig. 8 shows the present-day distribution of black hole mass, stellar halo mass, and metallicity for EAGLE central galaxies resident in MW-sized dark matter haloes. We split the sample according to the lookback time to the last merger with a satellite at least as massive as the SMC (stellar mass 5×10^8 $M_\odot$; McConnachie 2012).

There is a clear correlation between galaxy properties and lookback time to the last SMC-like merger. The trend is strongest for the mass and metallicity of the stellar halo. Fewer recent mergers imply a lower total number of mergers, a lower stellar halo mass, and a tendency for the halo to have been built by mergers with low-mass dwarf galaxies (Deason et al. 2016), which are more metal poor than more massive dwarfs (Kirby et al. 2013). The dependence of black hole mass on the time since the last merger is more complex because the black hole growth depends not only on the number of mergers, but also on the amount of gas available in the central galaxy. A more recent merger means, on average, fewer such mergers at high redshift when there was more gas available, while no mergers within the last 10 Gyr means fewer mergers overall, and hence fewer opportunities to trigger black hole growth.

Fig. 8 shows that a lack of SMC-like mergers in the past 10 Gyr results in systematically lower black hole masses and less massive and more metal-poor stellar haloes. This is consistent with the current state of the MW and suggests that the lack of significant satellite mergers in the past 10 Gyr is a likely explanation for why our galaxy is an outlier in scaling relations (see also Amorisco 2017b). This is consistent with recent analyses of *Gaia* DR2 data which suggest that today's MW halo is dominated by stars from a single SMC-mass galaxy which merged with our galaxy roughly 10 Gyr ago (Belokurov et al. 2018; Helmi et al. 2018).

5 DISCUSSION AND CONCLUSION

This study was motivated by a desire to understand the physical reason why the MW is an outlier amongst galaxies of similar stellar mass in three important properties: the mass of its central black hole, and the mass and metallicity of its stellar halo. These atypical properties could be due to a lack of significant mergers within the last ∼10 Gyr, with observations suggesting that since $z \sim 2$ the MW stellar halo has grown slowly through minor mergers (e.g. Deason et al. 2013; Deason et al. 2016; Amorisco 2017a,b). This hypothesis is supported by our analysis of the EAGLE hydrodynamical simulation, which predicts that MW-mass galaxies that have not recently experienced a merger with a galaxy more massive than the SMC have systematically smaller black holes and lower mass and more metal-poor stellar haloes, just like our own MW galaxy. Furthermore, Amorisco (2017b) showed that hosts that have recently accreted massive satellites that are not yet disrupted, such as the LMC, are more likely to have a lower mass and more metal-poor stellar halo than the overall population of galaxies of similar mass. Eventually, the destruction of the massive satellite leads to an increase in the stellar halo mass and metallicity. The solution to the MW's atypical properties is provided by a fourth unusual feature of the MW: the presence of a satellite with a mass as large as the LMC's.

Using a semi-analytic orbital evolution model that includes the MW, the LMC, and Andromeda, we established that the LMC will likely merge with our galaxy in $2.4^{+1.2}_{-0.8}$ Gyr (68 per cent confidence level), where the confidence interval has been calculated using a large number of Monte Carlo realizations that account for uncertainties in the LMC proper motions and in the dark matter halo masses of the LMC, MW, and Andromeda. More than 93 per cent of the Monte Carlo realizations end up with a MW–LMC merger, and, furthermore, the merger is insensitive to the presence of An-

dromeda since most realizations predict a merger well before our massive neighbour comes within a distance of 300 kpc from the Galaxy.

The MW–LMC merger is an inevitable consequence of the large dark matter mass that the LMC appears to have. Even though the LMC is currently heading away from the MW, dynamical friction acting on such a heavy galaxy will cause its orbit rapidly to lose energy and, approximately a billion years from now, to turn around and head towards the centre where it is destined to merge in another 1.5 billion years or so. The high mass of the LMC halo inferred from dynamical considerations (Peñarrubia et al. 2016) is consistent with the fact that, in the EAGLE simulations, LMC-mass satellites that themselves have a satellite as massive as the SMC typically have a halo mass, $M_{200} = 3.0^{+0.7}_{-0.8} \times 10^{11}\,\mathrm{M}_{\odot}$, at infall.

A massive LMC alters the position and velocity of the MW barycentre which, in turn, affects the eventual encounter between the MW and Andromeda, as anticipated by Gómez et al. (2015) and calculated using a simplified model by Peñarrubia et al. (2016). Our model shows that the Andromeda collision will be less head-on than previously thought, and that Andromeda's tangential velocity with respect to the MW–LMC barycentre is higher than previously estimated, which is in better agreement with cosmological expectations (Fattahi et al. 2016). We find that the first encounter between the MW and Andromeda will take place in $5.3^{+0.5}_{-0.8}$ Gyr (68 per cent confidence level), which is at least 1.5 Gyr later than previous estimates.

To discover the likely outcome of the MW–LMC merger, we identified analogue systems in the EAGLE simulation and followed their evolution through the merger process. We selected analogues by matching the black hole, gas, and halo masses of the MW and the stellar mass of the LMC. The merger of LMC analogues leads to large growth in the black hole mass of the MW analogues, with a clear enhancement compared to a merger-free control sample. Most of the mass of the merging satellite is deposited in the stellar halo between 10 and 100 kpc from the central galaxy. The merger also imparts gravitational kicks to a significant number of stars in the central galaxy which join the stellar halo. The metallicity of the halo is greatly increased.

Grafting the results of the EAGLE MW–LMC analogues to the real MW we find that following the merger of the LMC the Galactic black hole mass will increase by a factor of between 1.5 and 8 (median value 2.5). The merger will not destroy the disc, and the Galactic bulge will hardly change. This is exactly the trend needed to bring our Galactic black hole on to the mean black hole–spheroid mass relation. Debris from the LMC merger will overwhelm the stellar halo, whose mass will increase by a factor of between 3 and 6 (median value 5). This will promote the MW from the galaxy with the lowest stellar halo mass to an average galaxy. The metallicity of the newly formed stellar halo will effectively be that of the LMC, which is on the high side (but within the scatter) of the observed stellar halo metallicities in galaxies similar to the MW. The collision with the LMC will have restored our Galaxy to normality.

The growth of the supermassive black hole following the future MW–LMC merger will trigger AGN activity and possibly generate jets which, in turn, can produce powerful γ-ray emission (e.g. Padovani et al. 2017). If energetic enough, γ-rays impinging on the Earth can cause mass extinctions by destroying the planet's ozone layer (Thomas et al. 2005). However, the Galactic AGN will not be powerful enough to deplete the Earth's ozone layer and is very unlikely to pose a serious danger to terrestrial life. The MW–LMC merger will gravitationally eject central disc stars into the halo. Is the Sun a potential victim? Thankfully, this seems unlikely, as only a few per cent of the stars at the position of the Sun in our MW–LMC analogues are kicked out into the halo.

ACKNOWLEDGEMENTS

We thank the anonymous referee for their insightful comments. We also thank Andrew Cooper, David Rosario, and Joop Schaye for very helpful discussions. MC and CSF were supported by the Science and Technology Facilities Council (STFC) [grant numbers ST/I00162X/1, ST/P000541/1]; CSF was supported, in addition, by an ERC Advanced Investigator grant, DMIDAS [GA 786910]. AJD is supported by a Royal Society University Research Fellowship. SM was supported by STFC [ST/F001166/1, ST/L00075X/1] and by Academy of Finland, grant number: 314238. This work used the DiRAC Data Centric system at Durham University, operated by the Institute for Computational Cosmology on behalf of the STFC DiRAC HPC Facility (www.dirac.ac.uk). This equipment was funded by BIS National E-infrastructure capital grant ST/K00042X/1, STFC capital grants ST/H008519/1 and ST/K00087X/1, STFC DiRAC Operations grant ST/K003267/1, and Durham University. DiRAC is part of the National E-Infrastructure.

REFERENCES

Amorisco N. C., 2017a, MNRAS, 464, 2882
Amorisco N. C., 2017b, MNRAS, 469, L48
Anglés-Alcázar D., Faucher-Giguère C.-A., Quataert E., Hopkins P. F., Feldmann R., Torrey P., Wetzel A., Kereš D., 2017, MNRAS, 472, L109
Bell E. F., Monachesi A., Harmsen B., de Jong R. S., Bailin J., Radburn-Smith D. J., D'Souza R., Holwerda B. W., 2017, ApJ, 837, L8
Belokurov V., Erkal D., Evans N. W., Koposov S. E., Deason A. J., 2018, MNRAS, 478, 611
Besla G., Kallivayalil N., Hernquist L., Robertson B., Cox T. J., van der Marel R. P., Alcock C., 2007, ApJ, 668, 949
Binney J., Tremaine S., 2008, Galactic Dynamics, 2nd edn. Princeton Univ. Press, Princeton, NJ
Bland-Hawthorn J., Gerhard O., 2016, ARA&A, 54, 529
Boehle A. et al., 2016, ApJ, 830, 17
Bonaca A., Conroy C., Wetzel A., Hopkins P. F., Kereš D., 2017, ApJ, 845, 101
Booth C. M., Schaye J., 2010, MNRAS, 405, L1
Booth C. M., Schaye J., 2011, MNRAS, 413, 1158
Bower R. G., Schaye J., Frenk C. S., Theuns T., Schaller M., Crain R. A., McAlpine S., 2017, MNRAS, 465, 32
Brooks A., Christensen C., 2016, in Laurikainen E., Peletier R., Gadotti D., eds, Astrophysics and Space Science Library, Vol. 418, Galactic Bulges. Springer-Verlag, Berlin, p. 317
Brook C. B., Kawata D., Gibson B. K., Flynn C., 2004, MNRAS, 349, 52
Bullock J. S., Johnston K. V., 2005, ApJ, 635, 931
Callingham T. et al., 2018, preprint (arXiv:1808.10456)
Cooper A. P. et al., 2010, MNRAS, 406, 744
Cooper A. P., Parry O. H., Lowing B., Cole S., Frenk C., 2015, MNRAS, 454, 3185
Cox T. J., Loeb A., 2008, MNRAS, 386, 461
Crain R. A. et al., 2015, MNRAS, 450, 1937
D'Souza R., Bell E. F., 2018a, Nat. Astron., 2, 737
D'Souza R., Bell E. F., 2018b, MNRAS, 474, 5300
Deason A. J., Belokurov V., Evans N. W., Johnston K. V., 2013, ApJ, 763, 113
Deason A. J., Wetzel A. R., Garrison-Kimmel S., Belokurov V., 2015, MNRAS, 453, 3568
Deason A. J., Mao Y.-Y., Wechsler R. H., 2016, ApJ, 821, 5

Deason A. J., Belokurov V., Koposov S. E., Gómez F. A., Grand R. J., Marinacci F., Pakmor R., 2017, MNRAS, 470, 1259
Di Matteo T., Colberg J., Springel V., Hernquist L., Sijacki D., 2008, ApJ, 676, 33
Dubois Y., Volonteri M., Silk J., Devriendt J., Slyz A., Teyssier R., 2015, MNRAS, 452, 1502
Fardal M. A., Babul A., Geehan J. J., Guhathakurta P., 2006, MNRAS, 366, 1012
Fardal M. A. et al., 2013, MNRAS, 434, 2779
Fattahi A. et al., 2016, MNRAS, 457, 844
Font A. S., McCarthy I. G., Crain R. A., Theuns T., Schaye J., Wiersma R. P. C., Dalla Vecchia C., 2011, MNRAS, 416, 2802
Furlong M. et al., 2015, MNRAS, 450, 4486
Gaia Collaboration, 2018, A&A, 616, A12
Gilbert K. M. et al., 2014, ApJ, 796, 76
Gómez F. A., Besla G., Carpintero D. D., Villalobos Á., O'Shea B. W., Bell E. F., 2015, ApJ, 802, 128
Gómez F. A., White S. D. M., Marinacci F., Slater C. T., Grand R. J. J., Springel V., Pakmor R., 2016, MNRAS, 456, 2779
Gómez F. A., White S. D. M., Grand R. J. J., Marinacci F., Springel V., Pakmor R., 2017, MNRAS, 465, 3446
Goulding A. D. et al., 2018, PASJ, 70, S37
Guo Q., Cole S., Eke V., Frenk C., 2011, MNRAS, 417, 370
Harmsen B., Monachesi A., Bell E. F., de Jong R. S., Bailin J., Radburn-Smith D. J., Holwerda B. W., 2017, MNRAS, 466, 1491
Harris J., Zaritsky D., 2009, AJ, 138, 1243
Hayden M. R. et al., 2015, ApJ, 808, 132
Haywood M., Di Matteo P., Lehnert M. D., Snaith O., Khoperskov S., Gómez A., 2018, ApJ, 863, 113
Hellwing W. A., Frenk C. S., Cautun M., Bose S., Helly J., Jenkins A., Sawala T., Cytowski M., 2016, MNRAS, 457, 3492
Helmi A., Cooper A. P., White S. D. M., Cole S., Frenk C. S., Navarro J. F., 2011, ApJ, 733, L7
Helmi A., Babusiaux C., Koppelman H. H., Massari D., Veljanoski J., Brown A. G. A., 2018, Nature, 563, 85
Hernquist L., 1990, ApJ, 356, 359
Heyer M., Dame T. M., 2015, ARA&A, 53, 583
Hopkins P. F., Hernquist L., Cox T. J., Di Matteo T., Martini P., Robertson B., Springel V., 2005, ApJ, 630, 705
Jethwa P., Erkal D., Belokurov V., 2016, MNRAS, 461, 2212
Kallivayalil N., van der Marel R. P., Besla G., Anderson J., Alcock C., 2013, ApJ, 764, 161
Kallivayalil N. et al., 2018, ApJ, 867, 19
Kirby E. N., Cohen J. G., Guhathakurta P., Cheng L., Bullock J. S., Gallazzi A., 2013, ApJ, 779, 102
Kormendy J., Richstone D., 1995, ARA&A, 33, 581
Liu L., Gerke B. F., Wechsler R. H., Behroozi P. S., Busha M. T., 2011, ApJ, 733, 62
Magorrian J. et al., 1998, AJ, 115, 2285
McAlpine S. et al., 2016, Astron. Comput., 15, 72
McAlpine S., Bower R. G., Harrison C. M., Crain R. A., Schaller M., Schaye J., Theuns T., 2017, MNRAS, 468, 3395
McAlpine S., Bower R. G., Rosario D. J., Crain R. A., Schaller M., Schaye J., Theuns T., 2018, MNRAS, 481, 3118
McConnachie A. W., 2012, AJ, 144, 4
McMillan P. J., 2017, MNRAS, 465, 76
Merritt A., van Dokkum P., Abraham R., Zhang J., 2016, ApJ, 830, 62
Mihos J. C., Hernquist L., 1996, ApJ, 464, 641
Miyamoto M., Nagai R., 1975, PASJ, 27, 533
Monachesi A., Bell E. F., Radburn-Smith D. J., Bailin J., de Jong R. S., Holwerda B., Streich D., Silverstein G., 2016a, MNRAS, 457, 1419
Monachesi A., Gómez F. A., Grand R. J. J., Kauffmann G., Marinacci F., Pakmor R., Springel V., Frenk C. S., 2016b, MNRAS, 459, L46
Monachesi A. et al., 2018, preprint (arXiv:1804.07798)
Navarro J. F., Frenk C. S., White S. D. M., 1996, ApJ, 462, 563
Navarro J. F., Frenk C. S., White S. D. M., 1997, ApJ, 490, 493
Padovani P. et al., 2017, A&AR, 25, 2
Patel E., Besla G., Sohn S. T., 2017, MNRAS, 464, 3825
Peñarrubia J., Gómez F. A., Besla G., Erkal D., Ma Y.-Z., 2016, MNRAS, 456, L54
Pillepich A., Madau P., Mayer L., 2015, ApJ, 799, 184
Planck Collaboration I, 2014, A&A, 571, A1
Qu Y. et al., 2017, MNRAS, 464, 1659
Robotham A. S. G. et al., 2012, MNRAS, 424, 1448
Rodriguez-Gomez V. et al., 2016, MNRAS, 458, 2371
Rosas-Guevara Y., Bower R. G., Schaye J., McAlpine S., Dalla Vecchia C., Frenk C. S., Schaller M., Theuns T., 2016, MNRAS, 462, 190
Sales L. V., Navarro J. F., Kallivayalil N., Frenk C. S., 2017, MNRAS, 465, 1879
Savorgnan G. A. D., Graham A. W., Marconi A., Sani E., 2016, ApJ, 817, 21
Schaye J. et al., 2015, MNRAS, 446, 521
Shakura N. I., Sunyaev R. A., 1973, A&A, 24, 337
Shao S., Cautun M., Deason A. J., Frenk C. S., Theuns T., 2018, MNRAS, 479, 284
Sohn S. T. et al., 2017, ApJ, 849, 93
Thomas B. C. et al., 2005, ApJ, 634, 509
Tissera P. B., Scannapieco C., Beers T. C., Carollo D., 2013, MNRAS, 432, 3391
Trayford J. W. et al., 2015, MNRAS, 452, 2879
van der Marel R. P., Alves D. R., Hardy E., Suntzeff N. B., 2002, AJ, 124, 2639
van der Marel R. P., Fardal M., Besla G., Beaton R. L., Sohn S. T., Anderson J., Brown T., Guhathakurta P., 2012a, ApJ, 753, 8
van der Marel R. P., Besla G., Cox T. J., Sohn S. T., Anderson J., 2012b, ApJ, 753, 9
van der Marel R. P., Fardal M. A., Sohn S. T., Patel E., Besla G., del Pino-Molina A., Sahlmann J., Watkins L. L., 2018, preprint (arXiv:1805.04079)
Volonteri M., Haardt F., Madau P., 2003, ApJ, 582, 559
Wang W., White S. D. M., 2012, MNRAS, 424, 2574
Xue X.-X., Rix H.-W., Ma Z., Morrison H., Bovy J., Sesar B., Janesh W., 2015, ApJ, 809, 144
Zolotov A., Willman B., Brooks A. M., Governato F., Brook C. B., Hogg D. W., Quinn T., Stinson G., 2009, ApJ, 702, 1058

This paper has been typeset from a TEX/LATEX file prepared by the author.